

Determination of specular reflectances in a liquid medium with a variable angle of incidence

S. Gil, G. A. Clarke, L. McGarry, and C. E. Waltham

We present a technique we developed to measure specular reflectances of mirrors immersed in liquids and in air. The method works with a broad range of angles of incidence ($\theta = 15\text{--}75^\circ$). The wavelength range used in this research was from 250 to 800 nm, and the state of polarization of the incident rays could be continuously varied with respect to the phase of incidence. The technique used in this study is based on a low-cost variable angle reflectometer and a commercial spectrophotometer. Here we discuss the protocol we devised to extract reflectances with this instrument. This procedure was tested with samples that were measured through the use of ellipsometric techniques. The main advantages of the method discussed here are versatility, speed, and the availability of the equipment used; these are particularly useful for controlling the quality of a large number of samples. We present the results of reflectance measurements in water for dielectric coated aluminum intended for use in light concentrators for the Sudbury Neutrino Observatory. The error in our estimate of the overall reflectance, weighted over operational distributions of wavelength and incident angle, is $\pm 3\%$ for one sample and $\pm 5\%$ for the 2000 m² of coated material involved in this observatory.

1. Introduction

Determining the specular reflectances of materials is not easy, especially in liquid media that can damage reflectance standards. We were drawn to this problem during the development of light-concentrating reflectors for the Sudbury Neutrino Observatory (SNO). The SNO is a major new facility being constructed in Canada to detect neutrinos from the Sun and other astrophysical sources, such as supernovas.^{1,2} The detector consists of a spherical acrylic vessel containing 1000 tons of heavy water, surrounded by 6000 tons of light water (Fig. 1). Immersed in the light water are 9600 photomultiplier tubes (PMT's) to detect the blue and UV Čerenkov radiation produced by electrons and γ rays from neutrino interactions. So that the number of PMT's is reduced without compromising the efficiency of the detector, each PMT is surrounded by a light concentrator made from dielectric coated aluminum (DCA)

sheets that reflect light into the PMT (Fig. 2).³ These concentrators also have the desirable property of restricting the angle of acceptance of the PMT's. The cost of the light concentrators is small compared with that of the PMT's, which constitute a major fraction of the entire cost of the observatory.

One of the critical parameters in determining the efficiency of the SNO detector is the reflectance of the DCA. We need to know the reflectances in water, as a function of wavelength in the range of from 280 to 600 nm, and with a range of incident angles from 0° to 90° .⁴ The DCA consists of a highly polished aluminum sheet with a thickness of 0.3 mm,⁵ upon which the following proprietary coatings are evaporated: bonding aid and oxidation barrier, Al (primary optical surface), low refractive index layer ($n \approx 1.4$), and high refractive index layer and water seal ($n \approx 2.0$). The DCA was prepared by Optical Coating Laboratory, Inc. of Santa Rosa, California.⁶ The determination of the reflectance of the DCA was necessary for three reasons: (a) to maximize the light-collection efficiency of the SNO detector, (b) to satisfy the need for extensive quality control of the DCA to be used in the detector, and (c) to create a model that would allow us to predict reliably the reflectance characteristics of the DCA and thus the performance of the SNO detector.

Several experimental techniques have been devised for measuring the specular reflectance of mirror

When this research was performed the authors were with the Department of Physics, University of British Columbia, Vancouver BC, Canada V6T 1Z1. S. Gil is now with Departamento de Fisica, Comision Nacional de Energia Atomica, Av. del Libertador 8250, 1429 Buenos Aires, Argentina.

Received 14 October 1993; revised manuscript received 27 June 1994.

0003-6935/95/040695-08\$06.00/0.

© 1995 Optical Society of America.

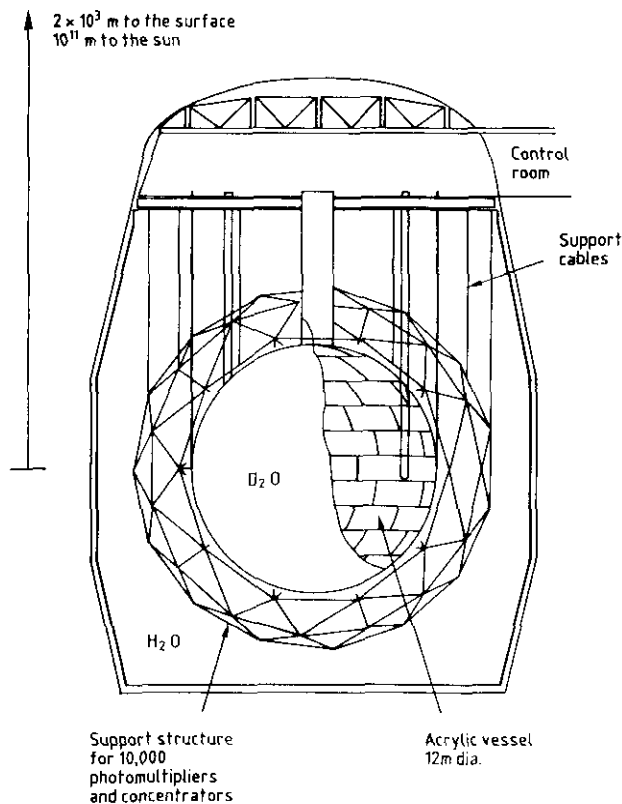


Fig. 1. Schematic diagram of the SNO detector.

samples in air.^{7,8} We have developed a technique to make measurements in water by using a commercially available spectrophotometer and a variable-angle reflectometer that was built in our laboratory. The complete range of wavelengths, polarization, and angles used in this study can be determined quickly. Nevertheless, important precautions must be taken in order to extract reliable specular reflectances. In the first part of this paper we describe the experimental techniques we used to develop a reliable protocol for obtaining specular reflectances. We then discuss how the determination of the experimentally obtained reflectance is used to obtain a model parameterization of the DCA. We also discuss the implica-

tion of the present measurements regarding the efficiency of the SNO detector.

2. Specular Reflectometer

The reflectometer we used in this study consists of a watertight Al box that fits into the sample receptacle of a Perkin-Elmer Lambda 3B ultraviolet-visible (UV-VIS) double-beam spectrophotometer. The reflectometer intercepts only one of the beams. It has two windows, as illustrated in Fig. 3, for light entry and exit. These are made of 1.5-mm-thick fused silica. The incident beam is reflected by a 90° mirror prism, which has a front-surface Al coating. The beam then strikes a rotatable reflectance accessory that contains two mirrors that form a 90° angle. The intersection of the two mirrors coincides with the axis of rotation of this accessory, and it is parallel to the edge of the 90° prism.

The rotating accessory is formed by a permanent front-surface Al mirror and the sample mirror. This latter mirror is supported by three rest points, which can be adjusted so that the two mirrors are precisely perpendicular to each other. The alignment of the complete assembly is accomplished by use of a laser beam. Invariance of the beam direction to better than 1 mrad is easily achieved with this reflectometer. Conceptually, this reflectometer is similar to a model that is commercially available through Perkin-Elmer that operates in air. As the accessory rotates, the position of the beam on the two mirrors also changes; therefore, the reflectances measured here are average properties of a region approximately 0.5 cm² of both of the samples. For the type of measurements used in this study, this feature is not a limitation.

In front of the entrance window, and mounted on the spectrophotometer itself, we placed an UV dichroic polarizer. This polarizer can be rotated continuously, but in practice two polarization orientations are used: *s*, with the electric field perpendicular to the plane of incidence, and *p*, with the electric field in the plane of incidence. Because of the large absorption of the polarizer in the far-UV region, this polarizer cannot be used below 300 nm. The use of a polarizer in the measurements of reflectances is

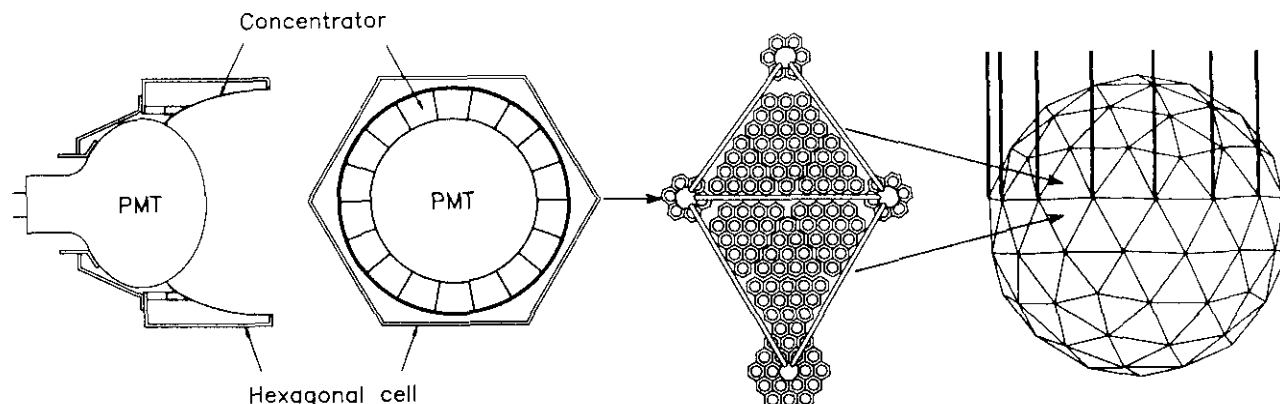


Fig. 2. Arrangement of the PMT's and DCA concentrators.

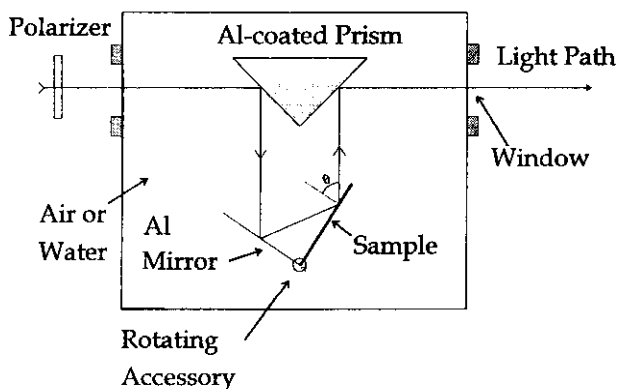


Fig. 3. Schematic diagram of the variable-angle reflectometer used in this study. The fluid container box was made of Al, and the entrance and exit windows were made of fused silica. The rotating accessory is attached to a goniometer to measure the angle of incidence, θ .

crucial when one is interested in determining reflectances at large incident angles, because in these cases the reflectances for the s and p states can be very different.⁷ Furthermore, the state of polarization of the incident beam of most spectrophotometers has considerable variation as a function of the wavelength. This variation in polarization is due to the multiple reflections that the incident beam undergoes within the monochromator of the spectrophotometer. In our particular case, we have measured the variation in polarization of the incident beam by using two types of polarizer: a dichroic polarizer and a Glan-Taylor polarizer. The latter polarizer has the advantage of having an excellent transmission in the range of $\lambda = 250\text{--}800$ nm, as well as a high degree of polarization purity. Unfortunately, because of its relatively large dimensions, it cannot be used in conjunction with the reflectometer. By comparing the transmission in the spectrophotometer, without and with the polarizer in the two orientations of interest (s and p), we were able to obtain the state of polarization of the incident beam. The results are shown in Fig. 4. For the region in which the dichroic polarizer has a good transmission, $\lambda > 300$ nm, the results of both polarizers are in excellent agreement. In this study we define the polarization angle, α , as the angle between the normal to the plane of incidence and the plane of the electric-field vector of the incident beam. Therefore, the s state corresponds to $\alpha = 0^\circ$ and the p state to $\alpha = 90^\circ$. Consequently, the probability of having a p component in the incident beam, P_p , is equal to $\sin^2(\alpha)$. The probability of having an s component, P_s , is equal to $\cos^2(\alpha)$. These parameters of the spectrophotometer (P_s and P_p) are useful for comparing the experimental values of reflectance with theory when the polarizer cannot be used, as is the case when $\lambda \leq 300$ nm.

3. Determination of Reflectances

We purchased from Labsphere, Inc.⁹ specular reflectance standards with known reflectances as a function of wavelength. We calibrated these primary

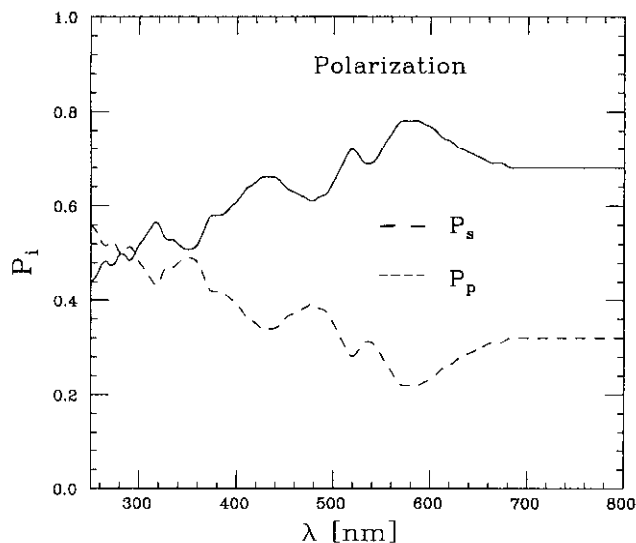


Fig. 4. State of polarization of the incident beam of the Perkin-Elmer Lambda 3B spectrophotometer as a function of wavelength. Quantity $P_s(P_p)$ is the probability of the component $s(p)$ in the incident beam.

reflectance standards against a master standard (produced by the National Research Council of Canada) by using an integrating sphere reflectometer with an incident angle of 8° . These primary reflectance standards are usually calibrated at a single angle and in air. Because the microstructure of a front-surface mirror standard is not well known, it is not possible for it to be used as a reference for other angles of incidence or for media different from air. Also, to avoid possible damage or alteration in the reflectance of our primary reference standards caused by immersion in water, we prepared secondary standard mirrors for immersion by evaporating Al (99.99% pure) onto glass substrates. To determine the reflectance of these secondary reflectance standard mirrors, $R_{\text{sec}}^{\text{air}}(\lambda)$, at each wavelength, λ , we calibrated them against the primary reflectance standards purchased from Labsphere. For this we used an integrating sphere reflectometer with an incident angle of 8° attached to a Beckman UV5270 spectrophotometer.

The secondary standard was also studied through the use of ellipsometric techniques, as we discuss in the following section. This method allowed us to determine the complex index of refraction of the Al as well as the index of refraction and thickness of the natural Al_2O_3 layer. Thus we were able to develop a model of reflectance for the secondary standard. The results of the model were then compared with the independent measurement of reflectances by use of the Labsphere standard at 8° . These results are displayed in Fig. 5. These two approaches agree within 1%, except at $\lambda < 300$ nm, where the agreement is only within 5%. Furthermore, the model of reflectance for the secondary standard allowed us to extend the values of the reflectances to other angles of incidence, within the same range of wavelength for which the ellipsometric studies were carried out. The model of reflectance was used to obtain the

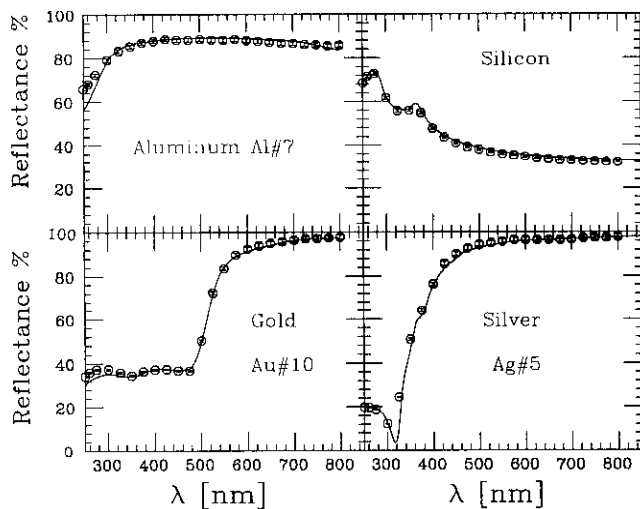


Fig. 5. Polarization average reflectance of samples of Al, Au, Si, and Ag. The Si sample was made of a finely polished Si wafer; the other samples were produced by evaporation in vacuum onto glass substrates. The circles are results obtained by use of an integrating sphere reflectometer with an incident angle of 8° , attached to a Beckman spectrophotometer. The curves are theoretical expectations for the reflectance at 8° , using a model for each sample obtained with the results of the ellipsometric studies.

transformation factors for converting the results of the measured reflectances at 8° to other incident angles explored in this study.

It is important to note that the change in the polarization average reflectances, $\langle R_{\text{sec}}^{\text{air}} \rangle(\lambda, \Theta)$, for the secondary standard is less than 3% within the range of λ and Θ encompassed in this study. Reasonable variation of the model for the secondary standard produced similar transformation factors. In fact, we estimate that $\langle R_{\text{sec}}^{\text{air}} \rangle(\lambda, \Theta)$ is known to within 1%. This is because the ratio of reflectances, $\langle R_{\text{sec}}^{\text{air}} \rangle(\lambda, \Theta) / \langle R_{\text{sec}}^{\text{air}} \rangle(\lambda, \Theta = 8^\circ)$, changes within approximately 1% for a range of models that are consistent with both the measurements of reflectances at 8° and the results of our ellipsometric studies. The reflectance in water for the secondary standard, $\langle R_{\text{sec}}^{\text{water}} \rangle(\lambda, \Theta)$, was obtained in a similar manner. With the notation $R_{\text{sample}}^{\text{medium}}(\lambda, \Theta, \text{pol})$, we denote the reflectance of the sample at the angle of incidence Θ , wavelength λ , and polarization state $\text{pol} = s$ or p . The superscript word medium stands for either water or air. Similarly, $RR_{\text{sample}}^{\text{medium}}(\lambda, \Theta, \text{pol}) [RR_{\text{sec}}^{\text{medium}}(\lambda, \Theta, \text{pol})]$ represents the values of the relative reflectance measured directly with the spectrophotometer.

The protocol used to extract the reflectance for a given sample consisted of measuring the relative reflectances, $RR_{\text{sample}}^{\text{medium}}(\lambda, \Theta, \text{pol})$, of the sample and the secondary standard, $RR_{\text{sec}}^{\text{medium}}(\lambda, \Theta, \text{pol})$, under exactly the same geometry and polarization state. The reflectance, $R_{\text{sample}}^{\text{medium}}(\lambda, \Theta, \text{pol})$, of the sample was then calculated as

$$R_{\text{sample}}^{\text{medium}}(\lambda, \Theta, \text{pol}) = R_{\text{sec}}^{\text{medium}}(\lambda, \Theta, \text{pol}) \frac{RR_{\text{sample}}^{\text{medium}}(\lambda, \Theta, \text{pol})}{RR_{\text{sec}}^{\text{medium}}(\lambda, \Theta, \text{pol})}, \quad (1)$$

where $R_{\text{sec}}^{\text{medium}}(\lambda, \Theta, \text{pol})$ is the value of the reflectance from the model for the secondary standard. Specifically, this model is used to calculate the transformation factor for obtaining $R_{\text{sec}}^{\text{medium}}(\lambda, \Theta, \text{pol})$ from the measured value $\langle R_{\text{sec}}^{\text{air}} \rangle(\lambda, \Theta = 8^\circ)$.

4. Specular Reflectance Calibration and Tests

To test the validity and accuracy of the technique proposed here, we performed independent reflectance measurements, coupled with analytical determinations of reflectances derived from ellipsometric studies, on the following test samples: silicon, gold, and silver. The last two were prepared by evaporating Au and Ag in vacuum onto glass substrates. The results of the ellipsometric tests allow us to model the different mirrors and compare their results with our reflectance determination. The results are presented in Fig. 5. These tests indicate the general agreement between our experimental technique and the model of reflectance constructed with the information from the ellipsometric studies. This experimental technique for measuring reflectance is standard and reliable. We performed several sets of measurements by using two different types of spectrophotometers, which gave results in agreement with each other to within 1%; therefore, the discrepancies observed are likely to be a consequence of the rather simple model used. Several additional tests were carried out to assess the soundness of the method used in this study. In particular, we have performed the following studies on our Si sample.

A. Polarization Test in Air

Using the standard (dichroic) polarizer, we measured reflectances of this sample in the two polarization states, s and p . From these measurements we extracted the average reflectance, $\bar{R}_{\text{sample}}^{\text{medium}}(\lambda, \Theta)$, defined as

$$\bar{R}_{\text{sample}}^{\text{medium}}(\lambda, \Theta) = \frac{1}{2} [R_{\text{sample}}^{\text{medium}}(\lambda, \Theta, s) + R_{\text{sample}}^{\text{medium}}(\lambda, \Theta, p)]. \quad (2)$$

We also determined ratio R_s/R_p as a function of wavelength for several angles of incidence. In Figs. 6 and 7 we show the result of our measurements, together with the expectations from a model of reflectance obtained from the ellipsometric studies on this sample. We see that the model and the measurements show the same trends, and that the average reflectances are in good agreement for all the angles. For ratio R_s/R_p the agreement is not as good, especially at the larger incident angles, but the trend is well reproduced.

Weighted Averages and Water Test

When the polarizer is not used in the reflectometer, it is important to recall that the incident beam of the spectrophotometer is partially polarized (see Fig. 4). To compare the results of the measurements with the theoretical expectation, we find it useful to introduce the concept of polarization average weighted reflectance

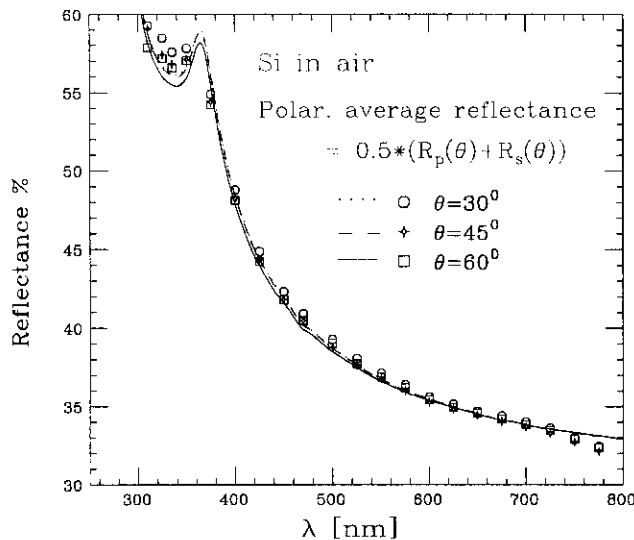


Fig. 6. Average reflectances of the Si sample in air for three angles of incidence. The curves are the predictions of the model derived from the ellipsometric studies.

tance, $\langle R \rangle_{\text{sample}}^{\text{medium}}(\lambda, \theta)$, defined as

$$\langle R \rangle_{\text{sample}}^{\text{medium}}(\lambda, \theta) = [R_{\text{sample}}^{\text{medium}}(\lambda, \theta, s)P_s(\lambda) + R_{\text{sample}}^{\text{medium}}(\lambda, \theta, p)P_p(\lambda)], \quad (3)$$

where $P_p(\lambda)$ and $P_s(\lambda)$ are the experimentally determined p and s components in the beam. Therefore, when it is necessary to study the reflectances of samples for $\lambda \leq 300$ nm, the polarizer has to be removed from the reflectometer. The results of the measurements are represented by the right-hand side of Eq. (3), whereas the left-hand side can be calculated by use of a model for the sample. The values of $\langle R \rangle_{\text{sample}}^{\text{medium}}(\lambda, \theta)$ for the sample of Si are shown in

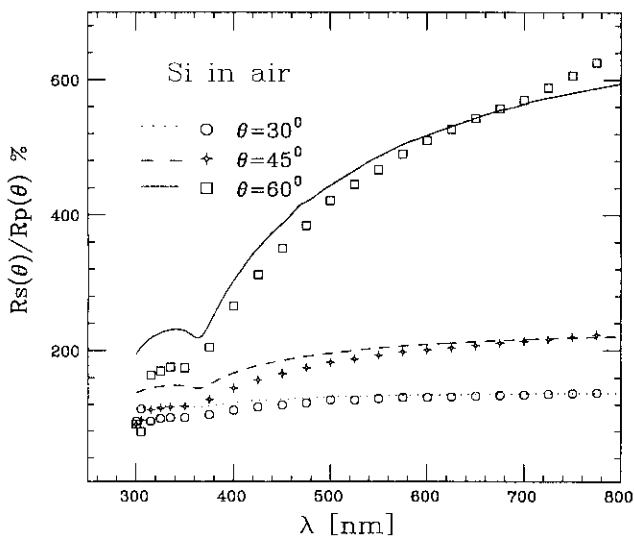


Fig. 7. Ratio of R_s/R_p for the Si sample in air for three angles of incidence. The curves are the predictions of the model derived from the ellipsometric studies.

Figs. 8 and 9 for measurements done in air and water, respectively. Again, in these figures we see good agreement between the result of the measurements and the expectation from the model. The trends are very well reproduced in all cases. All these tests give us confidence in the robustness of the present technique, but they also reveal its limitations. Some of the discrepancies between the results of our measurements and the predictions of the model used might likely originate in the simplicity of the model used to describe the ellipsometric result. A detailed comparison between the ellipsometric and reflectance measurements is beyond the scope of this study.

It is interesting to note that without the use of a reference standard with well-known reflectance properties, it is not possible to extract reliable information with this type of reflectometer. Usually the reflectances of the 90° prism and the permanent mirror that form the reflectometer are not known at all angles. Therefore the relative reflectances will depend on the properties of all the mirrors involved. The advantage of using the protocol proposed here is that by use of expression (1) the properties of the permanent mirror and the prism cancel out.

5. Ellipsometric Studies

Conceptually, an ellipsometer is an instrument that determines the complex reflectance ratio, $\rho = r_p/r_s$, of a sample surface. Here r_p and r_s are the complex reflectance for the p and s components. The connection with the previously defined reflectances, R_p and R_s , is

$$R_p = |r_p|^2, \quad R_s = |r_s|^2. \quad (4)$$

The spectroscopic rotating analyzer ellipsometer used in this study has been described in the literature.¹⁰

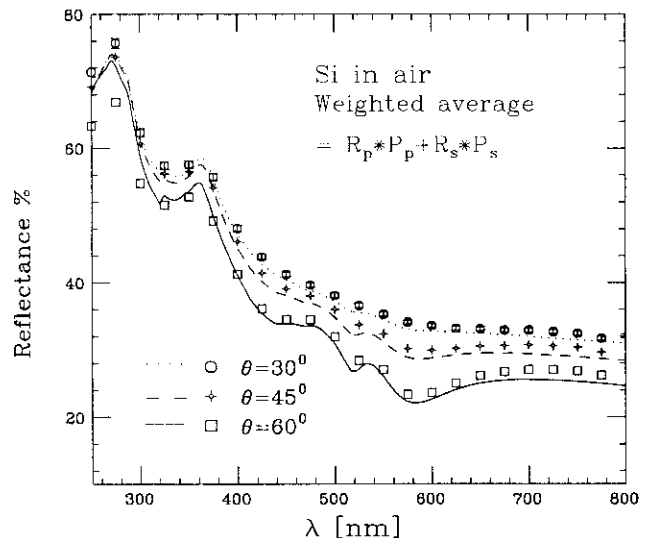


Fig. 8. Polarization average weighted reflectances of the Si sample in air for three angles of incidence. The curves are the predictions of the model derived from the ellipsometric studies. No polarizer is used in this case, making it possible to extend the measurements to wavelengths shorter than 300 nm.

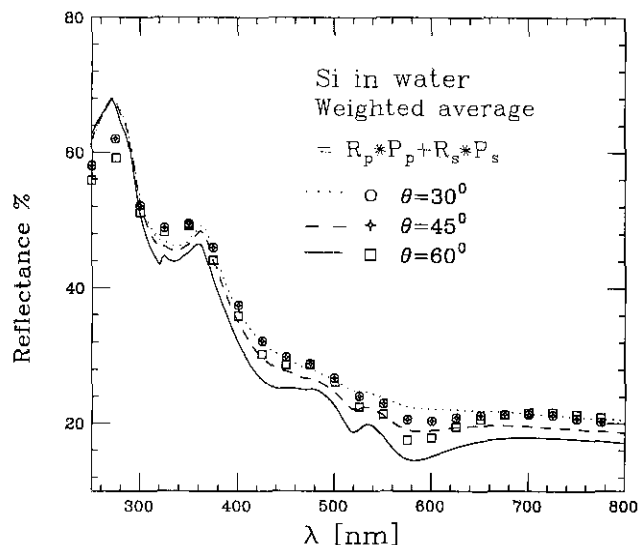


Fig. 9. Polarization average weighted reflectances of the Si sample in water for three angles of incidence. The curves are the predictions of the model derived from the ellipsometric studies.

This instrument contains a 75-W xenon arc lamp that provides a continuous broadband spectrum from 185 nm into the infrared. During operation, light of the desired wavelength is selected through the use of a double-prism monochromator and is linearly polarized after passing through a Rochon beam-splitting polarizer. The light beam is then reflected off the sample at an angle of incidence of 67.50° and passes through a rotating analyzer (a second Rochon polarizer). The intensity of the light on exit from the analyzer is measured with a PMT.

The theoretical value of ρ can be calculated through an n -layer model,¹¹ where the Bruggman effective medium theory¹² is used to model the complex index of refraction (or dielectric function¹³) of each layer. Therefore, the model parameters are the thicknesses of each layer and their complex indices of refraction. The analyzed Si sample consisted of a highly polished (111) silicon wafer. The model that provided the best fit consisted of a SiO_2 overlayer, 1.1 ± 0.1 nm in thickness, on pure silicon (Fig. 10). This model is then used to predict the reflectance of the Si sample (Figs. 5-9).

From our studies of the Al sample used as a secondary standard mirror, an excellent fit of ellipsometer results was obtained, assuming that this sample consists of only two layers: a thin film of Al_2O_3 (5.6 ± 0.3 nm in thickness) on top of a mixed layer of Al and 12% (in volume) Al_2O_3 , with refractive indices taken from Ref. 14. This model is then used to extract the reflectance of the secondary standard in air at 8° (Fig. 5), as well as the transformation function for obtaining the reflectances at other angles of incidence and also in water. Similarly, the solid curves in Fig. 5 for the Ag and Au samples were obtained through the use of a model obtained from this type of ellipsometric study. The effect of silver

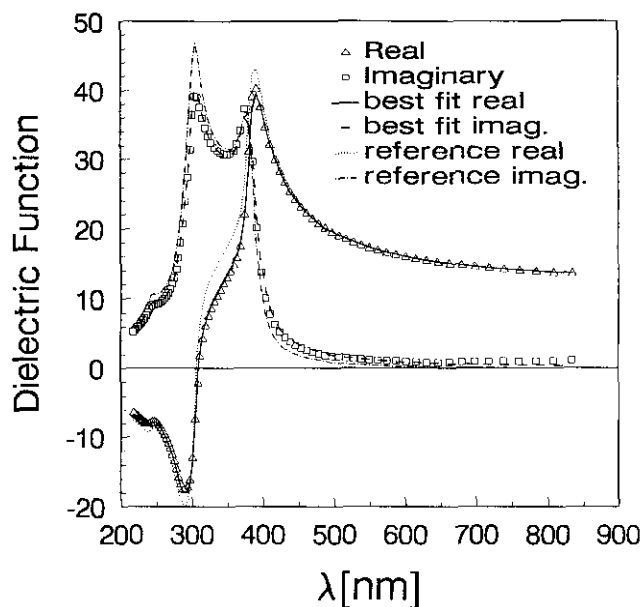


Fig. 10. Results of the ellipsometric measurements of the pseudo-dielectric function for the Si sample. The reference curves are the results obtained by use of the index of refraction for pure silicon. The best-fit curves were obtained with the assumption that the sample had a natural overcoat of SiO_2 of 1.1 nm.

tarnish was modeled with the interband method of Ref. 15.

One may assume that an ellipsometric study of this type could also be carried out for the DCA, therefore providing the necessary information for the calculation of the reflectances at the various angles of incidence and media. This procedure is indeed possible in principle, but in practice, because of the multiple layers involved (three) and the uncertainties in the indices of refraction involved, it is not possible to obtain as good a fit as in the cases of the simple mirrors described above. Therefore we chose to make a direct measurement of the reflectances for the DCA.

6. Determination of the Reflectance of the Dielectric Coated Aluminum in the SNO Concentrators

Using our reflectometer immersed in de-ionized water, we performed several series of measurements on different DCA samples. The measurements were conducted at $\theta = 20^\circ, 30^\circ$, and from 40° to 75° in steps of 5° in the wavelength range of 250 to 800 nm in the two polarization modes, s and p . The results for a typical sample are presented in Fig. 11. The distribution of angles of incidence was provided by Monte Carlo simulation: $W_{MC}(\theta)d\theta$ is the fraction of Čerenkov photons striking the concentrators with angles of incidence between θ and $\theta + d\theta$. The results of these simulations are shown in Fig. 12.

To evaluate the impact of the reflectance of the DCA on the efficiency of the SNO detector, we find it useful to define a mean reflectance (averaged over the operational distribution of incident angles),

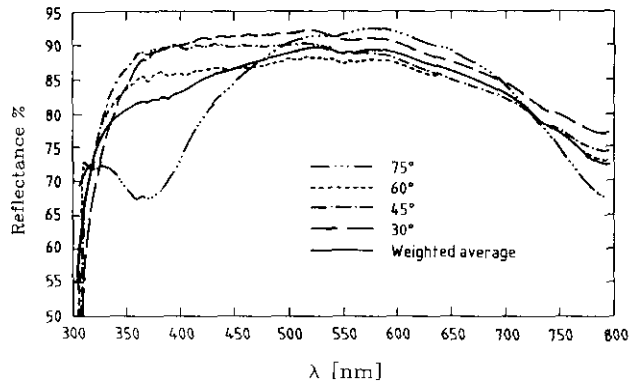


Fig. 11. Polarization averaged reflectance of a typical DCA sample immersed in ultrapure water for various angles of incidence. The weighted average is for the operational distribution of incidence angles encountered in the SNO detector (see Fig. 12).

$\langle R_{\text{DCA}}^{\text{water}} \rangle_{\theta}(\lambda)$, as

$$\langle R_{\text{DCA}}^{\text{water}} \rangle_{\theta}(\lambda) = \frac{\int_0^{90^\circ} \bar{R}_{\text{DCA}}^{\text{water}}(\lambda, \theta) W_{\text{MC}}(\theta) d\theta}{\int_0^{90^\circ} W_{\text{MC}}(\theta) d\theta} \quad (5)$$

In our case this integration is carried out numerically.

7. Determination of a Merit Factor for the Concentrator Samples

To determine the optimum coating thickness and to characterize the effect of the reflectance of the DCA on the efficiency of the SNO detector, we define the following merit factor function:

$$\text{MFF}(\lambda, d_{\text{acryl}}) = \langle R_{\text{DCA}}^{\text{water}} \rangle_{\theta}(\lambda) W(\lambda, d_{\text{acryl}}). \quad (6)$$

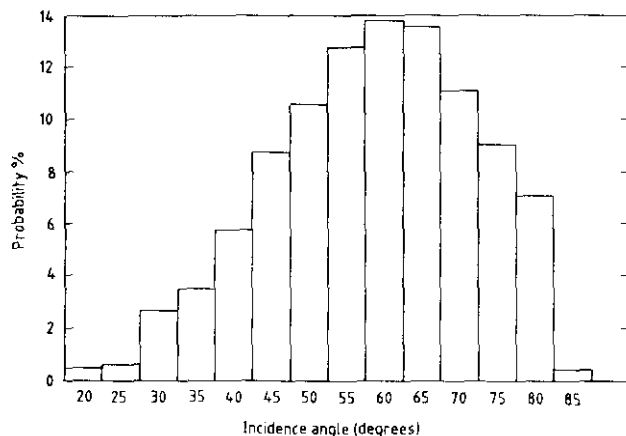


Fig. 12. Effective angular distribution of the incident photons on the light concentrators of the PMT of the SNO detector, $W_{\text{MC}}(\theta)$. These are the results of simulations that used the actual geometry of the concentrators.

The weighting function, $W(\lambda, d_{\text{acryl}})$, is defined by

$$W(\lambda, d_{\text{acryl}}) = \epsilon_{\text{PMT}}(\lambda) \frac{1}{\lambda^2} T_{\text{acryl}}(\lambda, d_{\text{acryl}}), \quad (7)$$

where $\epsilon_{\text{PMT}}(\lambda)$ is the PMT quantum efficiency, which was measured at Queen's University (PMT type R1408, serial number ZW531).¹⁶ Factor $1/\lambda^2$ describes the spectral distribution of the Čerenkov light.¹⁷ Quantity $T_{\text{acryl}}(\lambda, d_{\text{acryl}})$ describes the optical transmission of the acrylic in water and depends on the type of acrylic and the thickness of the acrylic vessel, d_{acryl} , as follows:

$$T_{\text{acryl}}(\lambda, d_{\text{acryl}}) = \exp[-\Lambda_{\text{acryl}}(\lambda) d_{\text{acryl}}], \quad (8)$$

where $\Lambda_{\text{acryl}}(\lambda)$ is the linear absorption coefficient for the acrylic. The values of this absorption coefficient for the specific type of acrylic used in the SNO detector were provided by researchers at Chalk River.¹⁸ The acrylic thickness used in our calculation was $d_{\text{acryl}} = 10$ cm, which is in accordance with the SNO design.

We also introduce the merit factor parameter (MF), defined as

$$\text{MF} = \frac{\int \langle R_{\text{DCA}}^{\text{water}} \rangle_{\theta}(\lambda) W(\lambda, d_{\text{acryl}}) d\lambda}{\int W(\lambda, d_{\text{acryl}}) d\lambda} \quad (9)$$

The validity of this factor relies on the result from simulations that the average number of reflections from a concentrator surface made by any photon generated throughout the active volume of the SNO detector is very close to one. The integrals are carried out over the relevant wavelength range of 250 to 700 nm. Therefore, the MF describes the fraction of the total number of photons detected by each concentrator-PMT unit compared with that of a similar PMT unit with an acceptance area equal to that of the concentrator. There is a variation of the weighted mean reflectances among the samples of approximately 5%. The manufacturers quote tolerances of 15% on the coating thicknesses for this large production run of approximately 2000 m². Although this has little effect on peak reflectances in the VIS range, our sensitivity to the position of the interference minimum in the UV causes this variation in weighted mean reflectance. In our case we found that $\text{MF} = 0.84 \pm 0.05$.

8. Summary

A reflectometer has been constructed for measuring specular reflectances in liquids as well as in air with a variable angle of incidence. The reflectometer is to be used in combination with a commercially available spectrophotometer. For reflectances to be extracted, a standard of known reflectance for each wavelength and angle is necessary. Standards were prepared,

their reflectances were measured against a commercially available reflectance standard, and their microstructures were studied through the use of ellipsometric techniques. This information allows us to predict the reflectances of the secondary standards at the various angles and in the different media used in this study. Typical uncertainties in the measurements of reflectance with the present technique are of the order of 3%. In addition, as the incidence angle changes, the position of the reflecting spot varies; therefore, the local variations of the sample are included in the measurements.

We have discussed the implications in terms of the impact of using dielectric coated aluminum to construct concentrators for the PMT's in the SNO detector. An overall mean reflectance of $84 \pm 5\%$ is expected for these concentrators. The concentrators will increase the total geometrical acceptance of the PMT's by a factor of 1.9. Thus the number of detected photons will increase by a factor of 1.6, with the mean number of reflections per photon being approximately 1.0. The expected cost increase caused by the concentrators is 6% of the PMT budget.

We thank J. Bosma for his fine craftsmanship in the construction of the reflectometer and J. Boyle for her assistance in the initial part of this project. We are grateful to M. Sirota for his valuable comments and suggestions in different parts of this study. We also thank G. Smith of Optical Coating Laboratories, Inc. for overseeing the production of our dielectric coated aluminum and for sharing with us his long experience with the material.

References

1. G. T. Ewan, "The Sudbury Neutrino Observatory," *Nucl. Instrum. Methods A* **314**, 373-379 (1992).
2. C. E. Waltham, P. Doe, R. G. H. Robertson, W. Frati, R. van Berg, K. T. Lesko, B. C. Robertson, and J. J. Simpson, "Research and development for the Sudbury Neutrino Observatory," *Phys. Can.* **48**, 135-141 (1992).
3. G. Doucas, S. Gil, N. A. Jelley, L. McGarry, M. E. Moorhead, N. W. Tanner, and C. E. Waltham, "Light concentrators for the Sudbury Neutrino Observatory," submitted to *Nucl. Instrum. Methods*.
4. G. Ouellette, C. E. Waltham, R. Meijer Drees, A. Poon, R. Schubank, and L. A. Whitehead, "Nonimaging light concentration using total internal reflection films," *Appl. Opt.* **31**, 2360-2365 (1992).
5. Alanod 310G electrolytically brightened anodized aluminum (anodized layer $2.0 \mu\text{m} \pm 10\%$ thick), from Alanod GmbH, Postfach 1102, D-5828 Ennepetal, Germany.
6. Optical Coating Laboratories Inc., Santa Rosa, Calif. 95401-7397.
7. G. Hass, J. B. Heaney, and W. R. Hunter, "Reflectometry," in *Physics of Thin Films* G. Hass, ed. Academic, New York, 1982), Chap. 12, pp. 1-51.
8. V. R. Weidner and J. J. Hsia, "NBS specular reflectometer-spectrophotometer," *Appl. Opt.* **19**, 1268-1273 (1980).
9. Labsphere, Inc., North Sutton, NH 03260.
10. B. T. Sullivan and R. R. Parsons, "A spectroellipsometric investigation of the effect of argon partial pressure on sputtered palladium films," *J. Vac. Sci. Technol. A* **5**, 3399-3407 (1987).
11. D. E. Aspnes, "Microstructural information from optical properties in semiconductor Technology," in *Optical Characterization Techniques for Semiconductor Technology*, D. E. Aspnes, R. F. Potter, and S. S. So, eds., *Proc. Soc. Photo-Opt. Instrum. Eng.* **276**, 188-195 (1981).
12. D. E. Aspnes, "Optical properties of thin films," *Thin Solid Films* **89**, 249-262 (1982).
13. D. E. Aspnes, "The accurate determination of optical properties by ellipsometry," in *Handbook of Optical Constants of Solids I*, E. Palik, ed. (Academic, New York, 1985), Chap. 5, pp. 89-112.
14. D. W. Lynch and W. R. Hunter, "The optical properties of metallic aluminum," in *Handbook of Optical Constants of Solids I*, E. Palik, ed. (Academic, New York, 1985), pp. 275-368.
15. A. R. Forouhi and I. Bloomer, "Calculation of optical constants, n and k , in the interband region," in *Handbook of Optical Constants of Solids II*, E. Palik, ed. (Academic, New York, 1985), Chap. 7, pp. 151-176.
16. H. B. Mak, Department of Physics, Queen's University, Kingston, Ontario, Canada K7L 3N6 (personal communication), 1992.
17. J. V. Jelley, *Čerenkov Radiation and Its Applications* (Pergamon, New York, 1958), Chap. I, p. 1.
18. E. Bonvin and E. D. Earle, Chalk River Laboratories, Chalk River, Ontario, Canada K0J 1J0 (personal communication), 1992.